Applied Geochemistry 81 (2017) 143–154

Contents lists available at ScienceDirect

Applied Geochemistry

journal homepage: www.elsevier.com/locate/apgeochem

Application of Portland cement to control acid mine drainage generation from waste rocks

Michael G. Sephton*, John A. Webb

Environmental Geosciences, La Trobe University, Melbourne, Victoria 3086, Australia

ARTICLE INFO

Article history:
Received 21 November 2016
Received in revised form
27 March 2017
Accepted 30 March 2017
Available online 31 March 2017

Editorial handling by Prof. M. Kersten.

Keywords:
Portland cement slurries
Acid mine drainage control
Oxygen consumption tests

ABSTRACT

Cement has been little investigated as a control for acid mine drainage, despite having advantages over cheaper alternatives. Leaching column experiments (set up in triplicate) investigated the effect of applying Portland cement slurries with three different water/cement (w/c) ratios (0.8, 1.0, 1.2) to pyrite-bearing waste rock from Brukunga mine in southeastern Australia. After application of the cement, leachate from the cemented columns showed a reduction in acidity compared to the control columns of ~85% and 100% for w/c ratios of 0.8 and both 1.0 and 1.2 respectively. This was due to direct neutralisation of acidity by cement dissolution and encapsulation of the pyrite-bearing rock fragments by the cement (as shown by a reduction in oxygen consumption rates of up to 70%). In columns with the higher w/c ratios (1.0, 1.2), the cement slurry penetrated to the base of the columns and greatly decreased the permeability. The greater coverage of the waste rock by the cement and increased contact time between the leachate and cement meant that no acid drainage leached from these columns (pH 7–8, Fe, Al, Mn, Zn and Cu concentrations rarely above detection limits). In columns with a w/c ratio of 0.8, the cement slurry was mostly retained in the upper 30–50% of the waste rock, leaving a large fraction of the waste rock below without any cement coverage. Leachate drained relatively quickly from these columns, probably through a small number of pathways through the cement plug and carried relatively small loads of acidity and metals from uncemented waste rock beneath the cement. Thus cement may be a viable method for controlling acid mine drainage generation from waste rock dumps, and could be applied with both lower and higher w/c ratios could be used to achieve an optimal balance between deep penetration and surficial retention.

1. Introduction

Acid mine drainage (AMD), which typically results from the oxidation of sulfide minerals in waste rock and tailings at mine sites, is an expensive environmental problem for the mining industry worldwide, as well as for governments managing historical mining landscapes (McCarthy, 2011; Harries, 1997; Nordstrom, 2011). A wide range of technologies has been developed for treating acid mine drainage (Lottermoser, 2003; Johnson and Hallberg, 2005; Blowes et al., 2003), but if the source is not effectively sealed from the atmosphere or from percolating water, then the need for treatment can remain for hundreds of years (Evangelou, 1995; Nieto et al., 2007). Controlling acid mine drainage at its source is challenging because the scale of the acid-generating waste deposits is often huge, in the order of millions of tons, and the cost can be very high, especially for historical mining landscapes where mine planning did not take AMD prevention into account (Davies et al., 2011; Edraki et al., 2005; Nordstrom and Alpers, 1999).

A variety of techniques have been tested and/or employed to control AMD at its source, including phosphate and silicate coatings (Evangelou, 1995; Mauric and Lottermoser, 2011; Ji et al., 2012; Kang et al., 2016) and the application of limestone (Lapakko et al., 1997; Miller et al., 2003, 2009) and alkaline industrial waste products such as fly ash (Canty and Everett, 2006; Perez-Lopez et al., 2007; Guynn, 2007; Hamel et al., 2010; Skousen et al., 2012), cement kiln dust (Doye and Duchesne, 2003; Duchesne and Doye, 2005; Sahoo et al., 2013), green liquor dregs (Ragnvaldsson et al., 2014) and bauxite residues (Doye and Duchesne, 2003; Duchesne and Doye, 2005; Maddocks et al., 2004).

Portland cement is produced by the calcination of limestone with a source of aluminosilicate (typically clay) at temperatures of around 1450–1500 °C (Hewlett, 1998), and is widely used for

---

* Corresponding author.
E-mail address: m.sephton@latrobe.edu.au (M.G. Sephton).

http://dx.doi.org/10.1016/j.apgeochem.2017.03.017

geotechnical stabilisation in mining and civil engineering, as well as in the encapsulation of hazardous wastes (Heinz, 1998; Sariosseiri and Muhunthan, 2009; Kogbara et al., 2013; Sheshpari, 2015). However, it has been rarely used or tested as a means of controlling or neutralizing AMD (Ji et al., 2012; Northwest Geochem, 1996,,Shabalala et al., 2017), even though it contains a similar amount of alkalinity as limestone, and (unlike limestone) forms a hard paste upon hydration with considerable impermeability (Banthia and Mindess, 1989; Claisse et al., 1999), which might be put to good effect in controlling AMD.

Furthermore, Portland cements can be applied via a range of different techniques including shotcreting, soilcreting and grout injection (Northwest Geochem, 1996; Spence, 1987), and with a wide range of water/cement ratios, which control the rheology of the slurry and the eventual distribution of cement through a rock mass (Axelsson and Gustafson, 2007; Heinz, 1998). Unlike clay cover systems, which require waste rock surfaces to be accessible to heavy vehicles, cement does not require compaction to set, and therefore could be applied to steep slopes of waste rock dumps, as well as being injected to encapsulate sulphide minerals buried deeply.

Thus there is much scope for research on the application of Portland cement to the problem of AMD. In this study, Portland cement slurries with three different w/c (water/cement) ratios were applied to sulphide bearing waste rocks from Brukunga, South Australia, to test the effectiveness of Portland cement in controlling AMD.

2. Materials and methods

2.1. Brukunga pyrite mine waste rocks

The Brukunga Pyrite Mine is located in the Adelaide Hills, 40 kms east of Adelaide in South Australia (Fig. 1). It was mined for sulfur from pyrite and pyrrhotite between 1955 and 1972 and produced around 8 million tonnes of waste rock, which remain exposed to the atmosphere at the site (Fig. 1, Taylor and Cox, 2003).

The mine was focused on the Nairne Pyrite Member within the shallow marine Cambrian Talisker Cal-siltstone; the sediments have been subjected to intermediate grade metamorphism and are now biotite-muscovite schists (Daily and Milnes, 1972) composed of quartz, feldspars (plagioclase and orthoclase) and mica (muscovite, biotite and phlogopite) (Ali, 2011). The ore consists of disseminated pyrite and pyrrhotite as well as veins of these minerals parallel to the bedding. A variety of secondary minerals (jarosite, alunite, rozenite, halotrichite, gypsum and elemental sulfur) has been identified at Brukunga (Agnew, 1994).

AMD produced by oxidation of sulphides in the waste rock dumps, quarry walls and tailings has been treated since 1980 in a lime neutralisation plant, which discharges neutral effluent from the mine to the downstream environment (Government of South Australia, Resources and Energy Group, 2014).

Approximately 90 kg of cobble-sized waste rocks were collected from three locations at the Brukunga mine on 24th June 2014: the southern waste rock dump, rubble beneath the high wall and a small pyramid-shaped dump used as a control in a previous field trial for cover techniques (Fig. 1).

2.2. Waste rock selection for leach columns

The rocks from each of the three different locations at the mine were crushed and sieved into fractions of 2–4.75 mm, 4.75–13.2 mm and 13.2–26 mm at Federation University in Ballarat, Victoria. Twelve 4.73 kg samples of waste rocks were assembled using the same proportions from each of the locations at the mine site (57.5% from the southern waste rock dump, 21.5% from the high wall and 21% from the small dump) and the same proportions of each of the different grain size fractions (14% in the 2–4.75 mm size fraction, 69% in the 4.75–13.2 mm size fraction and 17% in the 13.2–26 mm size fraction).

2.3. Leaching columns

Twelve leach columns, 15.5 cm in diameter and 28–34 cm long, were constructed from PVC pipe. A press-on cap with a tap was used to seal the column at the base, and a screw-on cap at the top. The 4.73 kg waste rock samples were poured from zip lock plastic bags into the columns.

2.4. Leaching regime

For the first leaching event, a 1 L graduated cylinder was used to pour enough deionized water into each column to fill it up to the brim (around 4 L). The volume of water added was used as a measure of the total void space in each column. For this initial leach, the taps at the bases of the columns were initially closed, allowing water to sit in the columns for 24 h to allow for dissolution of soluble salts that had accumulated since collection of the waste rocks. After 24 h, the taps were opened to allow for collection of the leachate in 1 L sample bottles.

The columns were subsequently leached with 1 L of deionized water approximately every two weeks over around six months (twelve times), and then kept dry for around 50 days, before the columns were leached one more time with 1 L of deionized water to remove soluble salts.

Cement treatments (see section 2.5 below) were then applied to 9 of the 12 columns in 3 groups of 3 (triplicates), with 1 set of 3 columns used as a control group (Table 1). Leaching commenced one week after the application of cement slurries; the columns were then leached approximately every two weeks over the next 5 months (a further nine times), and subsequently allowed to dry for around 50 days. Leaching every two weeks then resumed (nine times over around 5 months), before the columns were again left to dry for around 50 days. Finally, the columns were leached every two weeks for six weeks (three times) (see Fig. 2).

For each leaching application, the taps of the columns were opened, so that the leachate would drain freely through the waste rocks, and water was applied with pump action spray bottles to simulate rainfall. One day was allowed for the leachate to drain through the columns, before leachate samples were collected for analysis. The first time that the columns were leached after application of cement slurries, it was noted that rates of leachate drainage through some of the cemented columns decreased, therefore on this occasion, two days were allowed for leachate drainage. After the second column leach following cement application, rates of drainage had decreased even more, and so the time allowed for leachate drainage was extended to one week for the remainder of the experiment (Fig. 2). For those columns that drained very slowly, some water was retained on top of the cemented waste rock, and after each leachate sample was collected from these columns, the water retained was emptied, and its weight calculated from the difference between the weight of the column before and after emptying.

2.5. Cement application

The cement used was Cement Australia's General Purpose Cement, composed of 64.1% CaO, 19.7% SiO_2, 5.3% Al_2O_3, 2.7% Fe_2O_3, 1.6% MgO, 2.8% SO_3,0.7% K_2O and 0.1% Na_2O with an acid neutralizing capacity of 955 mg CaCO3 eq./g cement (see section 2.8). For

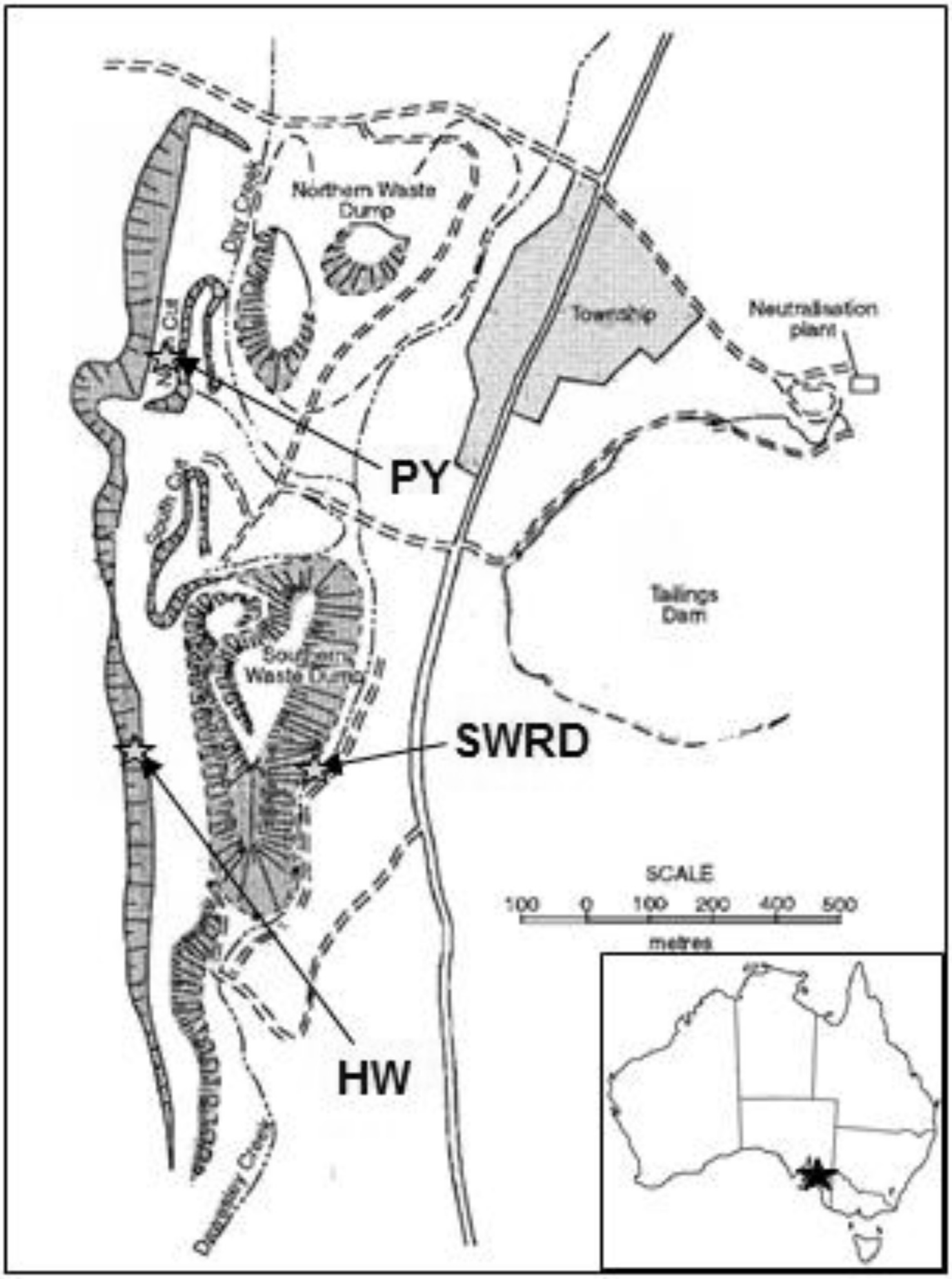

Fig. 1. Map of the Brukunga mine site with waste rock sampling locations: PY is the small pyramid shaped trial dump, SWRD is the southern waste rock dump and HW is the high wall (adapted from Agnew, 1994).

Table 1
Cement slurries applied to leach columns.

Columns	Treatment	Cement Composition	Water/Powder Ratio
1–3	Control	–	–
4–6	Cement	200 g water, 250 g cement	0.8
7–9	Cement	250 g water, 250 g cement	1.0
10–12	Cement	300 g water, 250 g cement	1.2

each column to which a cement slurry was applied, dry cement powder was weighed into a clean 2-L plastic beaker, mixed and pounded with a wooden spoon to ensure any lumps were broken up. The requisite mass of de-ionized water for the three w/c ratios tested (0.8, 1.0, 1.2; Table 1) was weighed into a clean 500 mL plastic beaker and added to the dry cement powder. The mixture was stirred vigorously to form a homogenous slurry, which was carefully poured over the rocks in the column, with the aim of achieving a uniform coverage over the waste rocks at the top of the column and as deep penetration as the rheological properties of the slurries and the permeability of the rocks would allow.

2.6. Analysis of leachates

The pH, redox potential and temperature of leachate samples were measured immediately following sample collection using TPS brand pH, redox and temperature sensors connected to a TPS WP-

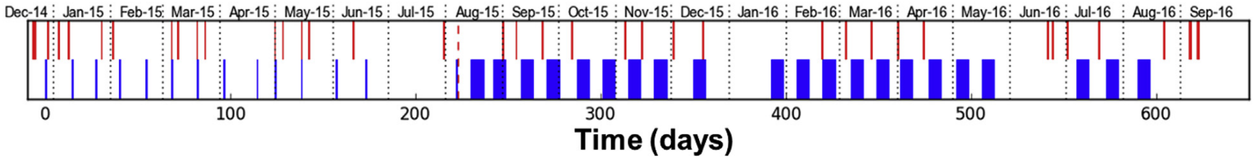

Fig. 2. Schedule used for oxygen consumption tests and column leaches. The time of cement application is marked with a dashed red line at 223 days. The upper bars in red are oxygen consumption tests and lower bars in blue are column leaches. The greater thickness of the blue bars after 223 days indicates the increased time allowed for leachate collection. (For interpretation of the references to colour in this figure legend, the reader is referred to the web version of this article.)

80D meter, and conductivity was measured using a TPS $k = 10.0$ type electrical conductivity sensor connected to a TPS AQUA-COND meter. Before use, the pH sensor was calibrated with $pH = 4$ and $pH = 7$ standards, the conductivity sensor was calibrated with a 2.76 mS/cm standard solution and the redox sensor was checked using Zobell's solution.

Acidity and alkalinity titrations were completed within a few days of sample collection using a Metrohm 888 Titrando autotitrator. Standards for alkalinity and acidity titrations were prepared by diluting laboratory reagent grade 0.1 M NaOH and 0.1 M HCl solutions from Chem-Supply Pty Ltd. to 1% in milliQ water, and then used to standardize the HCl and NaOH solutions for the alkalinity and acidity titrations respectively. Acidity titrations to a pH endpoint of 8.3 were carried out for leachate samples with $pH < 5$ using ~0.05 M NaOH. The sub-samples used for the titrations ranged in volume from 2 ml to 25 ml and were diluted to 50 ml with milliQ water, depending on the sample EC.

Alkalinity titrations to a pH endpoint of 3.5 were conducted on samples with $pH > 5$, using ~0.1 M or ~0.05 M HCl for samples with higher alkalinity and ~0.005 M HCl for samples with lower alkalinity. Alkalinity titrations were conducted using 50 ml unfiltered sub-samples of the collected leachates, except for the most alkaline leachates collected sooner after cement application, where the sub-sample volumes ranged from 1 to 10 ml and were diluted up to 50 ml with milliQ water. For the first leachate after cement application, alkalinity determinations performed on filtered leachate showed that unfiltered alkalinity was almost two times greater than the filtered alkalinity. The solids collected on the filter paper were white (not grey like cement) and most likely composed of precipitated calcite; they fizzed when treated with dilute HCl and saturation index (SI) calculations using PHREEQC (Parkhurst and Appelo, 2013) indicated these waters were highly oversaturated with respect to calcite ($SI > 2.5$).

Leachate sub-samples (~30 mL) were filtered through 0.45 μm nylon membrane filters, preserved with 0.5 %v/v concentrated nitric acid and stored at 4 °C. They were analysed for Fe, Al, Ca, Mg, Si, Mn, Cu, Zn and total S reported as SO_4^{2-} with a Perkin Elmer Optima 8000 ICP-OES after dilution with ~0.01 M nitric acid so that analyte concentrations were within the working range. Standards and quality control solutions were prepared from 1 g/L stock solutions of the elements analysed. Typical detection limits for Ca, Mg, Al, Fe, total S as SO_4^{2-}, Cu, Mn, Zn and Si as SiO_2 were 0.02, 0.13, 1.5, 0.24, 1.56, 0.01, 0.004, 0.019 and 0.14 mg/L respectively.

Na and K concentrations were determined using a Sherwood Model 420 Flame Photometer using filtered and acidified sub-samples ranging from 0.25 ml–4.5 ml. These samples were spiked with 0.5 ml of a 1 g/L Li stock solution to ensure each blank, standard and sample contained 100 mg/L Li as an internal standard and were diluted where necessary to a total of 5 ml. Detection limits for Na and K were 0.1 and 0.2 mg/L respectively. Fe^{2+} concentrations were determined from leachate samples from six columns, three times prior to the application of cements using the phenanthroline method with a LaMotte Smart3 colorimeter.

Prior to the application of cement to the leaching columns, the pH, EC and acidity of the leachates showed a low degree of variability, so only six of the thirteen leachate samples collected during this period were analysed for each of the 12 columns. Total loads for dissolved species in the leachate were calculated by scaling up the loads calculated using the six measured samples.

Ion chromatography (IC) was used for sulfur analysis after October 2015 in addition to ICP-OES, because sulfur analyses using ICP-OES on alkaline leachate samples tended to be unstable and yielded large charge balance errors, typically negative 20–40%. A major cause of these errors was likely due to the presence of low concentrations of hydrogen sulfide gas in the samples, resulting in higher sulfur intensities in the ICP-OES analysis (Colon et al., 2008), along with significant thiosulfate concentrations in some alkaline samples, identified with ion chromatography (discussed below). Charge imbalances in the first 2 or 3 leaches after cement application were also due to the use of unfiltered samples for alkalinity measurements, because calcite particles in the leachate dissolved during titration and resulted in overestimation of the alkalinity. This source of error was negligible after the 2nd or 3rd leach following cement application, because the measured alkalinities were very small compared to the sulfate concentrations.

In order to estimate the sulfate and thiosulfate concentrations of the alkaline samples collected between 15th August 2015 and 25th October 2015, these samples were treated with 1 drop of 35% H_2O_2 and re-analysed for total sulfur reported as SO_4^{2-} by ICP-OES in September 2016. The $S_2O_3^{2-}/SO_4^{2-}$ ratio for these samples was estimated based on trends in the $S_2O_3^{2-}/SO_4^{2-}$ ratios measured for the samples collected from the 8th November 2015 until the 9th August 2016, which were analysed using IC. Charge balance errors computed using the estimated $S_2O_3^{2-}$ and SO_4^{2-} concentrations based on the repeat analyses for total S were much lower than for those obtained using the original analyses.

Both sulfate and thiosulfate were analysed with a Metrohm Basic 883 Ion Chromatograph with a Metrosep A Supp 5–150/4.0 anion separation column. An eluent with 4 mmol/L Na_2CO_3 and 1 mmol/L $NaHCO_3$ with 10% acetone was used, and standards and quality control solutions were prepared from 1 g/L stock solutions using dried analytical grade Na_2SO_4 and $Na_2S_2O_3$ salts. 10% dilutions of the 1 g/L stock solutions were analysed with the ICP-OES to check the equivalence of the standards used for the IC with those used for ICP-OES. The 100 mg SO_4^{2-}/L solution was measured as 95 mg/L SO_4^{2-} while the 100 mg/L $S_2O_3^{2-}$ solution was measured as 172 mg/L SO_4^{2-} (100 mg/L S as $S_2O_3^{2-}$ is equivalent to 171 mg/L S as SO_4^{2-}).

Charge balance errors and saturation indices for all of the leachate samples were calculated using PHREEQC with the llnl.dat geochemical database. For over 90% of the leachate samples analysed (327 of 357), charge balance errors were within ± 10%.

2.7. Oxygen consumption tests

If sulfidic materials are oxidizing in a sealed container, the rate of decrease of partial pressure of oxygen gas may be useful as a quantitative indicator of the rate of sulfide oxidation, provided no other significant consumers or producers of oxygen are present

(Hollings et al., 2001; Lee et al., 2003; Song and Yanful, 2010).

The change in partial pressure of O_2 over time can be converted into the molar rate of O_2 consumption using the ideal gas law (Zumdahl, 1998):

$$V.dP_{O2}/dt = dn_{O2}/dt.R.T \quad (1)$$

where V is the volume of air in the container, dP_{O2}/dt is the rate of change of partial pressure of O_2 per unit time, dn_{O2}/dt is the rate of change of O_2 gas concentration in moles per unit time, R is the universal gas constant, and T is the temperature in degrees Kelvin.

The rate of O_2 consumption thus calculated can then be used to calculate the rate of SO_4^{2-} production using the stoichiometry of sulfide oxidation:

$$FeS_2 + 3.5O_2 + H_2O \rightarrow Fe^{2+} + 2SO_4{}^{2-} + 2H^+ \quad (2)$$

For each mole of pyrite oxidized, 3.5 mol of O_2 are consumed, and 2 mol of SO_4^{2-} are produced, so that the rate of SO_4^{2-} production can be calculated from the rate of O_2 consumption:

$$dn_{SO4}/dt = dn_{O2}/dt.2/3.5 \quad (3)$$

Oxidation of Fe^{2+} to Fe^{3+} may also contribute to the O2 consumption; colorimetric analyses showed that >90% of dissolved Fe in the leachates was Fe^{3+}.

$$Fe^{2+}0.5O_2(g) + 2H^+ \rightarrow Fe^{3+} + H_2O \quad (4)$$

This requires an additional 0.25 mol of O_2 per 2 mol of SO_4 produced, so that the relationship between SO4 production and O_2 consumption becomes:

$$dn_{SO4}/dt = dn_{O2}/dt.2/3.75 \quad (5)$$

The rate of SO_4^{2-} production calculated in this way can be compared with measured loads of SO_4^{2-} from the leachate analyses.

Oxygen consumption rates of the waste rocks in the leach columns were measured using six PASCO PASPORT Oxygen gas sensors (PS-2126A) with two PASCO Xplorer GLX dataloggers. Fifteen to seventeen measurements were completed on each column prior to the application of cements, and a further twenty measurements were completed on each column after the application of cements (Fig. 2).

Before each O_2 consumption measurement, the column was sealed by screwing on the cap tightly and closing the tap at the bottom. The oxygen gas sensor was inserted carefully into the hole in the column lid with a rubber stopper ring to ensure a tight seal, so that no significant gas exchange occurred between the atmosphere and the column air space.

The O_2 consumption tests were generally performed for a duration of around 24 h (minimum 12 h, maximum 60 h), and the logger was set to take measurements every 5 min for this duration. In order to complete the O_2 consumption measurements on the twelve columns using six O_2 sensors, the tests on the control columns and columns with cement with a w/c ratio of 1.0 were completed at the same time, and the tests on the columns with w/c ratios of 0.8 and 1.2 were one or two days later (depending on the duration of the first set of tests).

2.8. Analyses of cement powder and leached cement

To determine the chemical composition of the Portland cement used, the CaO, SiO_2, MgO, Al_2O_3 concentrations were determined using an Olympus DELTA-6000-C pXRF system and a sample of the cement prepared as a pressed pellet. A cement sample of known composition from Proficiency Testing Australia, prepared in the same manner, was also analysed, and the results used for calibration. Na and K concentrations in the Portland cement were determined with flame photometry, using 20% conc. HCl (2.4 M) and heat to digest the cement as described in Junsomboon and Jakmunee (2011). The acid neutralizing capacity of the dry cement powder was measured by digesting 2.0 g of cement in 60 ml of 1 M HCl on a hotplate at 90 °C for 2 h and performing a back-titration using ~0.05 M NaOH on an aliquot of the partially neutralised HCl (AMIRA International, 2002).

To identify any secondary minerals that formed within the cement during leaching, three cement samples were taken from one column (column 10, w/c = 1.2) 460 days after the cement was applied, ground to fine powder using a mortar and pestle, and analysed using a Siemens D5000 Diffractometer. Cu Kα radiation was used at 45 kV and 30 mA, over a 2θ range from 4° − 70°, with a step size of 0.02° and a 1 s time step.

3. Results and discussion

3.1. Oxygen consumption rates and leachate chemistry prior to cement application

Initial O_2 consumption rates prior to the first leach of the columns were low (Fig. 3b), likely due to lack of water or accumulated oxidation products on the sulfide mineral surfaces, inhibiting further sulfide oxidation (Jerz and Rimstidt, 2003). The first flush of the columns removed much of these oxidation products, and thus the leachate carried large loads of acidity (~13 g $CaCO_3$ equivalent) and concentrations of SO_4^{2-}, Fe, Al, Mg, Ca, Cu, Mn and Zn much higher than average levels measured once regular leaching commenced.

After the first leach, the O_2 consumption rates increased over the first 100 days (Figs. 3b), as did the concentrations of acidity, SO_4^{2-} and Fe (Fig. 3c and d, 4a). Total loads of acidity ranging from 50 to 65 g $CaCO_3$ equivalent were produced by the leach columns for the period after the first leach and prior to the application of cement at 223 days (Table 2).

The significant concentrations of Si, Al, Mg, Ca, Na and K in the leachate (Fig. 4a, b, c) are due to acid attack on silicate minerals in the waste rocks: phlogopite and biotite release K, Mg, Al and Si, and plagioclase releases Ca, Na, Al and Si.

3.2. Effects of cement application on waste rock permeability

After cement application, the columns with w/c = 0.8 cement addition continued to drain at around the same rate as the control columns; >90% of the applied 1 L of water was collected within minutes of application (~5 L/hr). In contrast, the columns with w/c = 1.0 and w/c = 1.2 cement additions drained slowly (4–17 ml/h).

The variability in permeability between the columns was due to differences in the penetration of the cement through the waste rocks. The higher w/c ratio (less viscous) cement slurries had penetrated all the way through the waste rocks and plugged the columns at the outlets (Fig. 5b and c), explaining the observed low permeability. In contrast the more viscous (w/c = 0.8) cement slurries were retained within the upper 30–50% of the waste rock mass (Fig. 5a), but left sufficient voids that water could flow quickly through the column via a reduced number of fluid pathways, as shown by the relatively fast rates of drainage through these columns (Fig. 3a).

Over the months following cement application, the rates of drainage in the columns with w/c = 1.0 and w/c = 1.2 cements decreased over time, as reflected by decreasing weights of leachate being collected (Fig. 3a). This decrease in permeability was probably due initially to increasing degree of cement hydration (Banthia

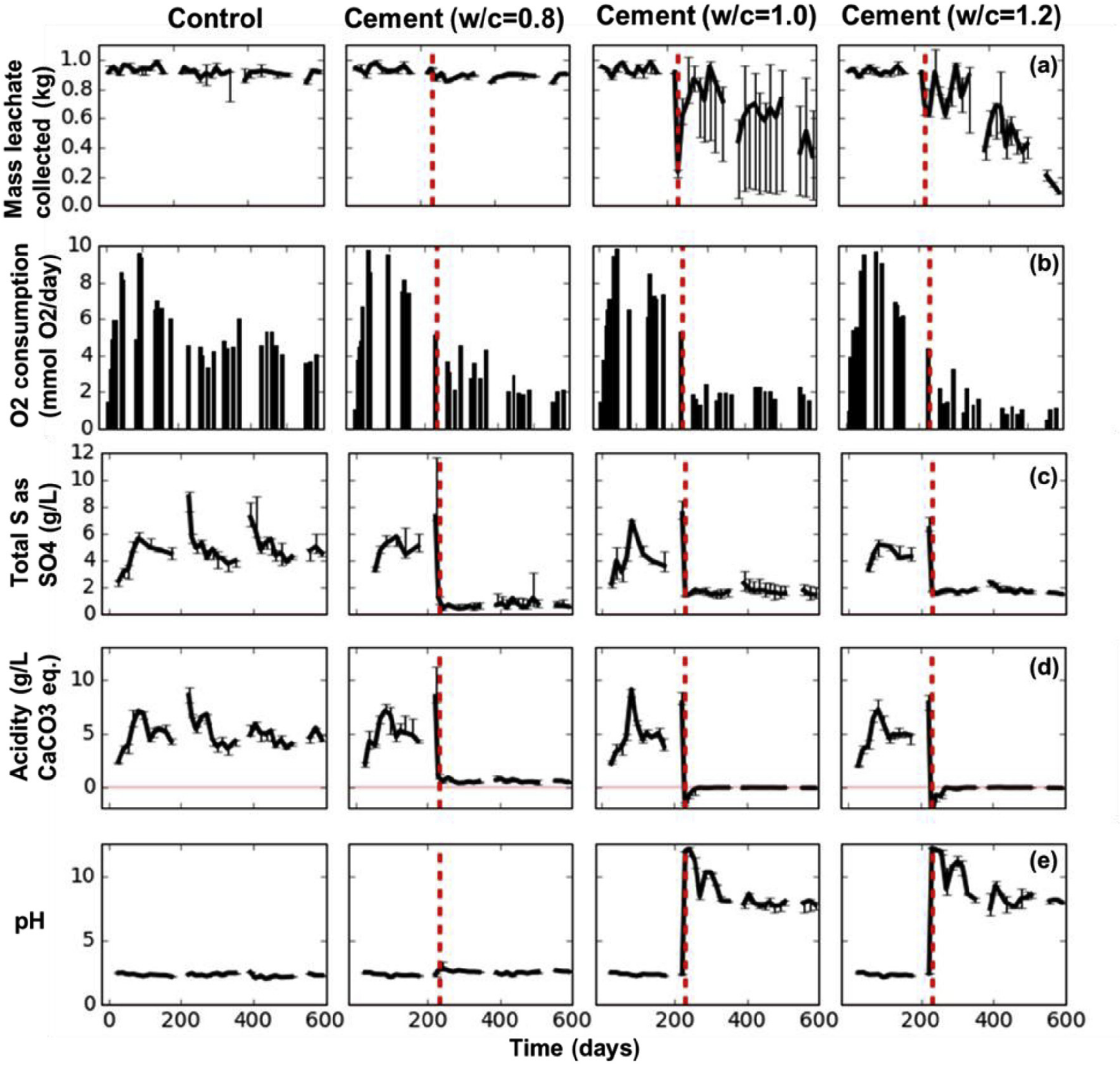

Fig. 3. Leach column results. a. Mass (kg) of leachate sample collected b. O2 consumption rates. Total S as SO_4^{2-} (g/L), d. Acidity (g/L $CaCO_3$ eq), e. pH. Data from the first flush at 0 days is omitted. Plotted values for each set of three columns are medians and the error bars mark the minimum and maximum values measured from each set of three columns. Lines are broken for the ~50 day dry periods (see section 2.4). Red dashed lines at 223 days mark the time at which cement slurries were applied. (For interpretation of the references to colour in this figure legend, the reader is referred to the web version of this article.)

and Mindess, 1989), and later to precipitation of secondary minerals, such as calcite ($CaCO_3$), gypsum ($CaSO_4.2H_2O$), ettringite ($Ca_6Al_2(SO4)_3(OH)_{12}\cdot 26H_2O$), thaumasite ($Ca_3Si(OH)_6(CO_3)(SO_4)\cdot 12H_2O$) and $Fe(OH)_3$ (Fig. 5d, Mikhail et al., 1981; Claisse et al., 1999) in pore spaces in the columns.

3.3. Effects of cement application on leachate chemistry

The divergence in permeability between columns with higher and lower w/c ratio slurries also manifested in the leachate chemistry (Table 3). The columns with cement applied at the lowest water/cement ratio (0.8) continued to produce acidic leachate, but exhibited a small increase in pH of around 0.3 units and the acidity was reduced by around 85% compared to the leachate from the control columns (Fig. 3d and e, Table 3). This reflected the relatively high viscosity of the cement slurry applied, such that it was retained in the upper part of the waste rock (section 3.2). The applied water quickly bypassed a significant fraction of the waste rock and incorporated acidity only from the uncemented waste rocks beneath, resulting in much reduced acidity, metal and total S loads (Table 3, Fig. 3c, d, f).

In contrast, the much more extensive distribution of cement and the lower permeabilities of the columns with higher w/c ratios resulted in very different leachate chemistry. These leachates initially had a very high pH of around 12 (Fig. 3e), high Ca (0.8–1 g/L) and alkalinity (Figs. 4b and 3d) and were highly oversaturated with respect to calcite (Fig. 4e), due to the rapid leaching of the small percent of calcium hydroxide produced by cement hydration (Taylor, 1997, p. 190). Within a few months, pH and alkalinity of these columns decreased to 7–8 and 20–50 mg/L $CaCO_3$ equivalent respectively (Fig. 3d and e). Ca concentrations remained at a relatively high level (~0.6 g/L, Fig. 4b) as did total S (~2 g/L, Fig. 3c), indicating that the cement was neutralizing sulfuric acid generated from pyrite oxidation in the waste rocks, and being depleted of calcium in the process.

Metal concentrations (Fe, Al, Cu, Mn and Zn) in leachate from the columns with high w/c ratios were only rarely above detection limits (Fig. 4a), due to four factors. The extensive distribution of cement through these columns resulted in decreased pyrite oxidation due to direct encapsulation of a large fraction of pyrite-

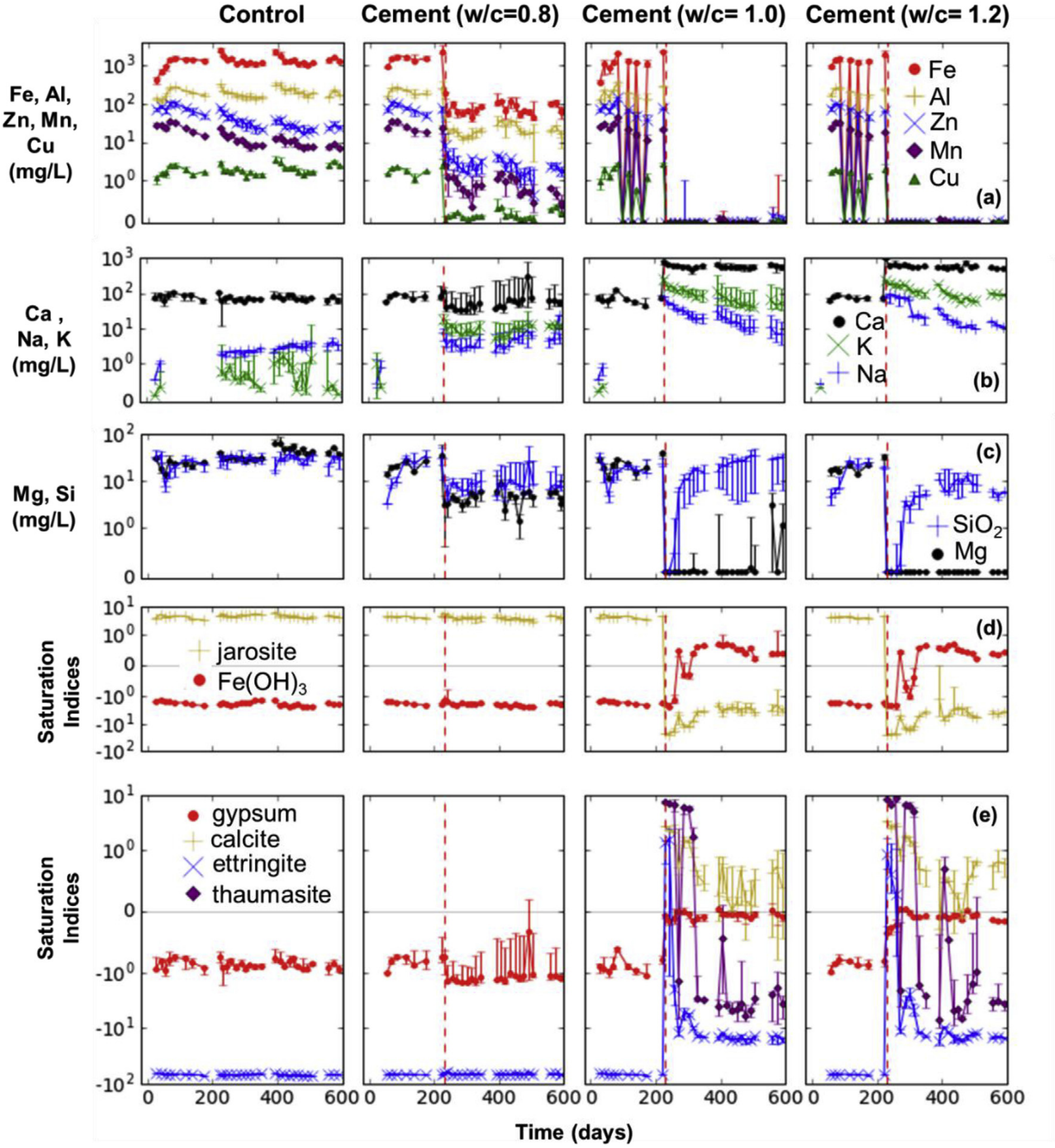

Fig. 4. Leach column results. a. Fe, Al, Zn, Mn, Cu (mg/L). b. Ca, Na, K (mg/L), c. Si, Mg (mg/L), d. Saturation indices for jarosite and $Fe(OH)_3$, e. Saturation indices for calcite, gypsum, ettringite and thaumasite. Values below method detection limits were plotted as 0. Plotted values for each set of three columns are medians and the error bars mark the minimum and maximum values measured from each set of three columns. Lines are broken for the ~50 day dry periods (see section 2.4). Red dashed lines at 223 days mark the time at which cement slurries were applied. Saturation indices for jarosite calculated using the method detection limit of 0.2 mg/L for K, for samples collected prior to cement addition, which were not analysed for K. Saturation indices for ettringite and $Fe(OH)_3$ were calculated using 50% of the method detection limits for Al (0.75 mg/L) and Fe (0.12 mg/L) respectively, when measured values were below the detection limits. (For interpretation of the references to colour in this figure legend, the reader is referred to the web version of this article.)

Table 2
Average hydrogen ion activity as pH and median annual mass fluxes of Ca, Mg, Al, Fe, S as SO_4^{2-}, Si as SiO_2, Cu, Mn, Zn and acidity for leachates samples calculated from loads measured from leachates collected over 223 days prior to application of cement slurries.

Columns	pH	S as SO_4^{2-} (g/yr)	Fe (g/yr)	Al (g/yr)	Ca (g/yr)	Mg (mg/yr)	SiO_2 (mg/yr)	Cu (mg/yr)	Mn (mg/yr)	Zn (mg/yr)	Acidity (g/yr)
1–3	2.36	92.0	25.1	4.1	1.7	549	493	37	496	1507	99.7
4–6	2.40	94.0	27.4	3.8	1.6	464	413	35	482	1487	102.9
7–9	2.37	86.0	23.9	3.9	1.5	503	404	32	485	1483	95.9
10–12	2.38	84.0	23.7	3.7	1.4	429	349	30	449	1370	100.4

bearing waste rock surfaces with cement (Fig. 5d, discussed further in section 3.4). Secondly, the rate of acid attack on the silicate minerals in the waste rock was greatly reduced due to the increased pH of the pore waters (Acker and Bricker, 1992; Gudbrandsson

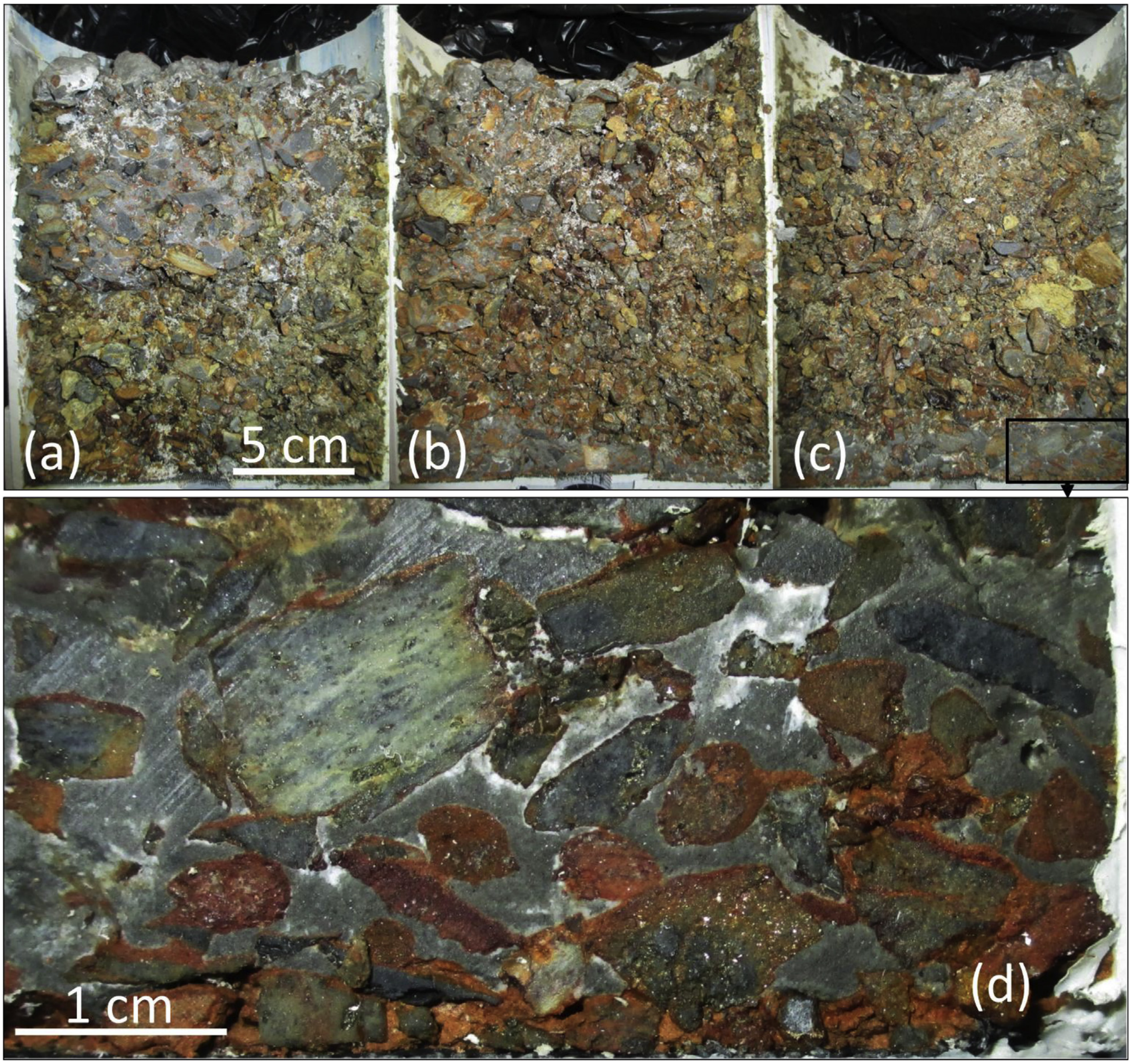

Fig. 5. Penetration of cement through the columns as shown by cross sections. a. w/c = 0.8, b. w/c = 1.0 and c. w/c = 1.2, d. Close-up of boxed area in (c), showing secondary mineral precipitates concentrated along waste rock/cement boundaries.

Table 3
Average hydrogen ion activity as pH and median annual mass fluxes of Ca, Mg, Al, Fe, S as SO_4^{2-}, Si as SiO_2, Cu, Mn, Zn, and acidity calculated from analyses of samples collected from leach columns over 360 days after the application of cement slurries.

Columns	Group	w/c ratio	pH	S as SO_4^{2-} (g/yr)	Fe (g/yr)	Al (g/yr)	Ca (g/yr)	Mg (mg/yr)	SiO_2 (mg/yr)	Cu (mg/yr)	Mn (mg/yr)	Zn (mg/yr)	Acidity (g/yr)
1–3	Control	n.a	2.29	93.2	26.0	3.8	1.4	778	591	40	195	589	92.1
4–6	Cement (w/c = 0.8)	0.8	2.57	14.9	1.6	0.4	1.7	99	191	3.6	17.3	50.1	10.9
7–9	Cement (w/c = 1.0)	1.0	7.9	26.2	0.0	0.0	9.1	3.3	301	0.07	0.21	0.56	−2.5
10–12	Cement (w/c = 1.2)	1.2	8.1	27.9	0.0	0.0	9.5	0	77	0.06	0.13	0.13	−3.7

et al., 2014), as shown by the very low levels of Mg released by biotite/phlogopite dissolution in the leachates from these columns (Fig. 4d). Thirdly, Fe^{2+}, Fe^{3+} and Al^{3+} have very low solubility at neutral to moderately alkaline pH and are removed by hydroxide precipitation (Stumm and Morgan, 1996, Chapter 6); red/orange ferric hydroxides are abundant in the cemented columns (Fig. 5d). Finally Cu, Mn and Zn were likely removed by sorption to the aforementioned Fe and Al hydroxides (McDonald et al., 2006; Langmuir, 1997, Chapter 10), and to the cement matrix (Haselbach et al., 2014).

The very different leachate chemistries also resulted in different secondary mineral assemblages. The acidic leachates characteristic of the control and w/c = 0.8 columns were saturated with respect to jarosite ($(K,Na)Fe_3(SO4)_2(OH)_6$) (Fig. 4d). The switch in leachate chemistry from acidic to alkaline that occurred upon cement application, especially for the columns with high w/c ratios, resulted in conversion of jarosite to $Fe(OH)_3$ (Fig. 4d), and increased the Na and K concentrations of the leachate (Fig. 4b). The higher pHs and concentrations of Ca, SO_4^{2-} and alkalinity in these leachates resulted in saturation with respect to calcite, gypsum, and briefly to thaumasite and ettringite after cement application (Fig. 4e). The precipitation of thaumasite immediately after cement application in the w/c = 1.0 and 1.2 columns is also indicated by the extremely low Si concentrations at this time (Fig. 4c). XRD analyses of three cement samples obtained from column 10 (w/c = 1.2) at 460 days after cement application confirmed the presence of calcite and gypsum.

3.4. Effect of cement application on sulfide oxidation

The O_2 consumption rates of the cemented columns declined compared to the controls after cement application (Fig. 3b), indicating that the cement caused a substantial drop in the rate of pyrite oxidation. The reduction in O_2 consumption and pyrite oxidation rates was gradual for the w/c = 0.8 columns, which for the first 6 months after cement application had relatively high O_2 consumption rates (Fig. 3b), probably because the limited cement penetration in these columns (Fig. 5a, section 3.2) left a large fraction of waste rock uncemented and free to oxidise. O_2 consumption for these columns then decreased significantly over time (Fig. 3b), indicating decreasing permeability of the cement to O_2; which may be partly due to an increase in the degree of cement hydration and partly due to secondary mineral precipitation within the cement matrix (section 3.2). The O_2 consumption rates approximately one year after cement application were around 50% of those measured in the control columns (Fig. 3b), reflecting the fact that 30–50% of the waste rocks were actually covered by cement (Fig. 5a). This indicates that the rates of sulfide oxidation in the cement-covered rocks at the top of the columns were probably very small, since the bulk of the observed O_2 consumption is likely to be occurring in the uncemented waste rocks beneath. The measured S mass flux from the columns was much less than the rate of SO42- production from pyrite oxidation calculated from the oxygen consumption rates (Fig. 6), indicating that the cement capping caused leachate flows to be concentrated along few fluid conduits, transporting pyrite oxidation products from a small fraction of the uncemented waste rock surfaces.

In the columns with higher w/c ratios (1.0 and 1.2), the total reduction in O_2 consumption and pyrite oxidation was greater (50–70%) and more sudden (Fig. 3b) because of the much deeper and more extensive distribution of cement through the waste rocks in these columns (Fig. 5b and c). The increased contact time between the leachate and waste rock surfaces due to the lower permeability of the columns resulted in a similar S mass flux as the rate of SO_4^{2-} production by pyrite oxidation, as evidenced by a good fit between measured S loads and those computed from the O_2 consumption rates (Fig. 6).

In laboratory-scale batch testing of the effectiveness of a range of coating agents in inhibiting sulfide oxidation, Ji et al. (2012) demonstrated that cement achieved the best effect, but remarked that cement may not be appropriate for field application because of the difficulty of distributing it to small pore spaces and deep voids within waste rock and tailings. However, the present study showed that cement application can significantly reduce sulfide oxidation rates and acidity generation even when not distributed deep into the waste rock, because it seals fluid pathways, so that a considerable fraction of the acid-producing waste rock is no longer in contact with water seeping through the material.

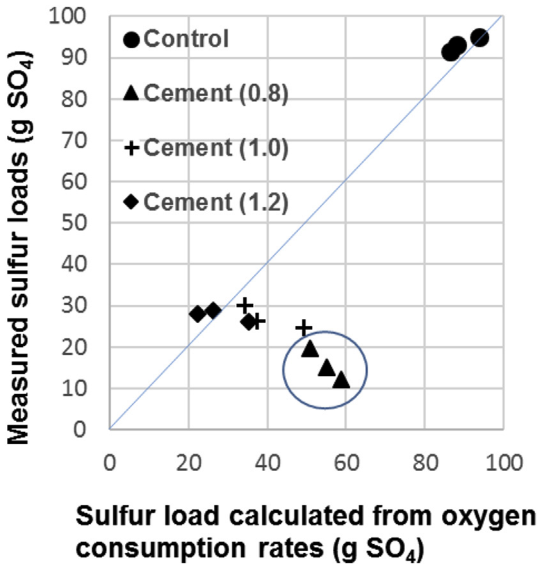

Fig. 6. Total measured S loads over 360 days after the application of cements compared against loads computed from measured O_2 consumption rates over the same period using equations (1) and (5) (section 2.7). Encircled outliers are from the columns with the lowest water/cement ratio (0.8). Blue line indicates an ideal case where the mass of S released is equal to the mass of S oxidized. (For interpretation of the references to colour in this figure legend, the reader is referred to the web version of this article.)

3.5. Rates of cement deterioration

The leachates from the cemented columns with w/c ratios of 1.0 and 1.2 have much greater Ca concentrations than those from the control columns, but similar Si concentrations to the controls (Fig. 4b and c, Table 4). This reflects incongruent dissolution of the Portland cement, whereby Ca depletion is favored and the Ca/Si ratio of the cement decreases over time (Harris et al., 2002). The leachates from the cemented columns with w/c = 0.8 have Ca concentrations similar to those in the leachates from the control columns, indicating much lower rates of cement dissolution (Fig. 5b, Table 3). This is probably due to the limited contact time between the leachate and the cement resulting from both the faster rates of drainage in these columns (section 3.2) and the lesser dispersion of the cements compared to the columns with higher w/c ratio cements (Fig. 5a–c).

Because Ca is the major soluble component of the cement, the rate of calcium depletion may indicate the effective longevity of the cements. The total loads of Ca measured in the leachates over 360 days of leaching amount to 1.5% of the total Ca mass originally

Table 4
Rates of depletion of Ca and Si from the cements.

	Total Ca, Si (g) in 250 g of cement added to column (see section 2.5)		Total Ca, Si load from leachates (g) after 360 days (Table 3)		% Ca, Si from cement depleted in first year	
	Ca	Si	Ca	Si	Ca	Si
Control	n.a	n.a	1.3	0.59	n.a	n.a
Cement (w/c = 0.8)	114	22.9	1.7	0.19	1.5%	0.8%
Cement (w/c = 1.0)	114	22.9	9.1	0.30	7.9%	1.3%
Cement (w/c = 1.2)	114	22.9	9.5	0.07	8.2%	0.3%

present in the cements for the w/c = 0.8 columns, and around 8% for the columns with w/c ratios of 1.0 and 1.2 (Table 4). If these rates of Ca loss remain constant, the Ca of the cements will be consumed after around 12.5 years for the columns with w/c ratios of 1.0 and 1.2 and 67 years for the columns with w/c ratios of 0.8 (Table 4).

These values are only indications of cement longevity, because there are several complicating factors. Firstly, rates of Ca loss and sulfide oxidation are unlikely to remain constant in the long term. Over time the sources of both Ca and S decrease, and this could cause dissolution rates to decrease.

Secondly but conversely, cement deterioration may expose pyrite surfaces and result in increased sulfide oxidation and acidity production over time, which in turn is likely to drive increased cement dissolution, such that leaching of both Ca and S would increase.

Thirdly, the rate of cement dissolution indicated by leaching of Ca is an underestimate of the true rate because some of the Ca released from the cement is retained within the columns in secondary Ca-bearing minerals such as calcite, gypsum, ettringite and thaumasite (section 3.3). Nonetheless, retention of Ca in these secondary minerals probably contributes to the lower permeability and lower sulfide oxidation rates of the cemented waste rock. Similarly, whilst the cement remains sufficiently alkaline, the solubility of iron will remain low at the sulfide mineral/cement interface, which will continue to be enriched with $Fe(OH)_3$, also contributing to the lower permeability and lower sulfide oxidation rates in the cemented waste rocks.

Finally, because some of the Ca in the leachate may originate from plagioclase weathering, as occurs in the control columns, the actual rates of cement dissolution may be lower than indicated by the Ca loads, although the rate of plagioclase weathering is likely to be very small in the columns with high w/c ratios (see section 3.3).

Therefore, the long-term trajectories of the rates of cement deterioration and sulfide oxidation are uncertain and longer term studies are necessary to obtain realistic estimates of the longevity of the cement treatments.

3.6. *Field application of cement to waste rock piles*

The results of this study demonstrate that applying Portland cement as a slurry to AMD-producing waste rock is effective in controlling AMD generation in different ways. High w/c ratios can be employed to achieve deep penetration of a waste rock dump, whereas slurries with lower w/c ratios can be used to cap the dump at the surface, sealing fluid pathways and minimizing infiltration. The technique of grout thickening, whereby the w/c ratio is decreased during the course of grout application (Axelsson and Gustafson, 2007), could be used to achieve an optimal balance between volume and density of the cement cap and to minimize water use.

4. Conclusions

A range of cement slurries was applied to acid mine drainage producing waste rocks in columns subjected to periodic leaching over 590 days, greatly diminishing acidity and metal loads (Fe, Al, Cu, Mn and Zn) and substantially reducing sulfide oxidation and S release.

For the cement applications with the lower w/c ratio of 0.8, the cement slurries were more viscous and cement was largely retained as a cap within the upper 30–50% of the waste rock profiles. The result of this cement coverage was little change in the bulk permeability of the waste rock and leachate remaining acidic, but with greatly reduced total S and acidity loads (by ~85%). The reduction in O_2 consumption rates (30–50%) was consistent with the coverage of cement through the waste rocks, indicating that the sulfide oxidation rate of the cement covered rocks was probably very small. The greater reduction in acidity loads than oxidation rates was likely due to the cement sealing fluid conduits and allowing only a small fraction of the waste rock surface areas to contribute to acidity loads.

For cement applications with a higher w/c ratio of 1.0 and 1.2, the cement slurries infiltrated the entire column depth, so the cement was distributed throughout the waste rocks, but concentrated at the base. The cement coverage reduced oxygen consumption rates by 50–70% and greatly decreased the permeability of the columns and the leachates were alkaline to neutral with zero acidity. Measured sulfur loads corresponded well with sulfur loads computed using oxygen consumption rate measurements, indicating that sulfate was being removed from the columns at a similar rate to the rate at which sulfate was being produced by pyrite oxidation.

Rates of cement deterioration indicated by Ca loads were much lower for the fast-draining columns with the lower w/c ratio (0.8) cements than for those columns with higher w/c ratios (1.0 and 1.2), which were less permeable. If the Ca mass fluxes from the cemented columns measured over approximately one year remained constant into the future, then the cements would likely remain effective for decades, although there are many uncertainties and longer term studies are necessary to obtain realistic estimates of the longevity of the cement applications.

In practice, both low and high w/c ratio slurries could be used together to achieve an optimal balance between penetration and dense coverage to minimize AMD generation from waste rock dumps.

Acknowledgements

Thanks to Andrew Forster, Diana Cato-Smith and Sam Sheppard for assistance with lab work, to Terry Ryan for building the leaching columns and leaching column stands, to Raul Mollehuara and Chris Henschke from Mineral Resources, South Australia for assistance with the collection of samples from the Brukunga Mine, to Bob Smith and Gordon Williams from Federation University, Victoria for assistance with crushing and sieving the waste rock samples, and to Jorg Metz for supplying the Proficiency Testing Australia cement standard. Thanks also to Charles Cravotta and Michael Kersten who reviewed this paper for providing valuable comments and suggestions. Michael Sephton was supported by an Australian Physiotherapy Association.

Appendix A. Supplementary data

Supplementary data related to this article can be found at http://dx.doi.org/10.1016/j.apgeochem.2017.03.017.

References

Acker, J.G., Bricker, O.P., 1992. The influence of pH on biotite dissolution and alteration kinetics at low temperature. Geochimica Cosmochimica Acta 45 (8), 3073–3092. http://dx.doi.org/10.1016/0016-7037(92)90290-Y.

Agnew, M., 1994. Weathering Products and Geochemistry of Waste Residues at the Brukunga Pyrite Mine, Adelaide Hills, S.a in Relation to Environmental Impacts (Honours thesis submitted to the University of Adelaide, South Australia, Australia).

Ali, F., 2011. Improving Understanding of the Geochemistry at the Brukunga Pyrite Mine, South Australia. Honours thesis submitted to La Trobe University, Victoria, Australia.

AMIRA International, 2002. ARD Test Handbook. Project P387A Prediction and Kinetic Control of Acid Mine Drainage. Ian Wark Research Institute and Environmental Geochemistry International Pty Ltd.

Axelsson, M., Gustafson, G., 2007. Grouting with High Water/solid-ratios – Literature and Laboratory Study. Department of Civil and Environmental Engineering, Division of GeoEngineering, Research Group of Engineering Geology, Chalmers University of Technology, Gteborg, Sweden. Report No. 2007:5.

Banthia, N., Mindess, S., 1989. Water permeability of cement paste. Cem. Concr. Res. 19 (5), 727–736. http://dx.doi.org/10.1016/0008-8846(89) 90043–4.

Blowes, D.W., Ptacek, C.J., Jambor, J.L., Weisener, C.G., 2003. 9.05- the geochemistry of acid mine drainage. In: Turekian, H.D.H.K. (Ed.), Treatise on Geochemistry, vol. 2003. Pergamon, Oxford, pp. 149–204.

Canty, G.A., Everett, J.W., 2006. Alkaline injection technology: field demonstration. Fuel 85 (17), 2545–2554. http://dx.doi.org/10.1016/j.fuel.2006.05.010.

Claisse, P.A., Elsayad, H.I., Shaaban, I.G., 1999. Permeability and pore volume of carbonated concrete. ACI Mater. J. 96 (3), 378–381.

Colon, M., Iglesias, M., Hidalgo, M., Todoli, J.L., 2008. Sulfide and sulfate determination in water samples by means of hydrogen sulfide generation- inductively coupled plasma- atomic emission spectrometry. J. Anal. Atomic Spectrom. 23, 416–418. http://dx.doi.org/10.1039/B716302A.

Daily, B., Milnes, A.R., 1972. Revision of the stratigraphic nomenclature of the Cambrian Kanmantoo group, South Australia. J. Geol. Soc. Aust. 19 (2), 197–202.

Davies, H., Weber, P., Lindsay, P., Craw, D., Pope, J., 2011. Characterisation of acid mine drainage in a high rainfall mountain environment, New Zealand. Sci. Total Environ. 409 (15), 2971–2980. http://dx.doi.org/10.1016/j.scitotenv.2011.04.034.

Doye, I., Duchesne, J., 2003. Neutralisation of acid mine drainage with alkaline industrial residues: laboratory investigation using batch-leaching tests. Appl. Geochem. 18 (8), 1197–1213. http://dx.doi.org/10.1016/S0883-2927(02)00246-9.

Duchesne, J., Doye, I., 2005. Effectiveness of covers and liners made of red mud bauxite and/or cement kiln dust for limiting acid mine drainage. J. Environ. Eng. 131 (8), 1230–1235. http://dx.doi.org/10.1061/(ASCE)0733-9372(2005)131:8(1230).

Edraki, M., Golding, S.D., Baublys, K.A., Lawrence, M.G., 2005. Hydrochemistry, mineralogy and sulfur isotope geochemistry of acid mine drainage at the Mt. Morgan mine environment, Queensland, Australia. Appl. Geochem. 20 (4), 789–805. http://dx.doi.org/10.1016/j.apgeochem.2004.11.004. April 2005.

Evangelou, V.P., 1995. Pyrite Oxidation and its Control. CRC Press, Inc., Boca Raton, FL.

Government of South Australia, Resources and Energy Group, 2014. Brukunga Mine Site Water Monitoring Report 2013. September 2014, Report Book 2014/00019.

Gudbrandsson, S., Wolff-Boenisch, D., Gislason, S.R., Oelkers, E.H., 2014. Experimental determination of plagioclase dissolution rates as a function of its composition and pH at 22 °C. Geochimica Cosmochimica Acta 139, 154–172. http://dx.doi.org/10.1016/j.gca.2014.04.028.

Guynn R.L. (2007) Use of CCP grout to reduce the formation of acid mine drainage: 10-Year update on the Winding Ridge Project. Proceedings of World of Coal Ash, May 7–10, Northern Kentucky, USA.

Hamel, B.L., Stewart, B.W., Kim, A.G., 2010. Tracing the interaction of acid mine drainage with coal utilization byproducts in a grouted mine: strontium isotope study of the inactive Omega Coal Mine, West Virginia (USA). Appl. Geochem. 25 (2), 212–223. http://dx.doi.org/10.1016/j.apgeochem.2009.11.006.

Harries, J., 1997. Acid Mine Drainage in Australia: its Extent and Potential Future Liability. Supervising Scientist Report 125. Australian Government Department of the Environment.

Harris, A.W., Manning, M.C., Tearle, W.M., Tweed, C.J., 2002. Testing of models of the dissolution of cements - Leaching of synthetic CSH gels. Cem. Concr. Res. 32 (5), 731–746. http://doi.org/10.1016/S0008-8846(01)00748-7.

Haselbach, L., Poor, C., Tilson, J., 2014. Dissolved zinc and copper retention from stormwater runoff in ordinary Portland cement pervious concrete. Constr. Build. Mater. 53, 652–657.

Heinz, W.F. (1998) Mining grouting in South African Deep Mines- Historical Overview and State-of-the-Art, Proceedings of International Mine Water Association Symposium Johannesburg 1998, pp. 121–140.

Hewlett, P.C. (Ed.), 1998. Lea's Chemistry of Cement and Concrete, fourth ed. Arnold.

Hollings, P., Hendry, M.J., Nicholson, R.V., Kirkland, R.A., 2001. Quantification of oxygen consumption and sulfate release rates for waste rock piles using kinetic cells: cluff lake uranium mine, northern Saskatchewan, Canada. Appl. Geochem. 16 (9–10), 1215–1230. http://dx.doi.org/10.1016/S0883-2927(01)00005-1. July 2001.

Jerz, J.K., Rimstidt, J.D., 2003. Pyrite oxidation in moist air. Geochem. Cosmochimica Acta 68 (4), 701–714. http://dx.doi.org/10.1016/S0016-7037(03)00499-X.

Ji, M., Gee, E., Yun, H., Lee, W., Park, Y., Khan, M., Jeon, B., Choi, J., 2012. Inhibition of sulfide mineral oxidation by surface coating agents: batch and field studies. J. Hazard. Mater. 229–230, 298–306. http://dx.doi.org/10.1016/j.jhazmat.2012.06.003.

Johnson, D.B., Hallberg, K.B., 2005. Acid mine drainage remediation options: a review. Sci. Total Environ. 338, 3–14. http://dx.doi.org/10.1016/j.scitotenv.2004.09.002.

Junsomboon, J., Jakmunee, J., 2011. Determination of potassium, sodium, and total alkalies in Portland cement, fly ash, admixtures, and water of concrete by a simple flow injection flame photometric system. J. Automated Methods Manag. Chem. 2011 http://dx.doi.org/10.1155/2011/742656. Article ID 742656.

Kang, C.U., Jeon, B.H., Park, S.S., Kang, J.S., Kim, K.H., Kim, D.K., Choi, U.K., Kim, S.J., 2016. Inhibition of pyrite oxidation by surface coating: a long-term field study. Environ. Geochem. Health 38 (5), 1137–1146. http://dx.doi.org/10.1007/s10653-015-9778-9.

Kogbara, R.B., Al-Tabbaa, A., Yaolin, Yi, 2013. Cement-fly ash stabilisation/solidification of contaminated soil: performance properties and initiation of operating envelopes. Appl. Geochem. 33, 64–75. http://dx.doi.org/10.1016/j.apgeochem.2013.02.001.

Langmuir, D., 1997. Aqueous Environmental Geochemistry. Prentice-Hall, Inc, Upper Saddle River, New Jersey, USA.

Lapakko, K., Antonson, D.A., Wagner, J.R., 1997. Mixing of limestone with finely crushed acid-producing rock. In: Proceedings of the Fourth International Conference on Acid Rock Drainage. Vancouver, B.C, Canada, pp. 1345–1360. May 31-June 6.

Lee, E.S., Hendry, M.J., Hollings, P., 2003. Use of O2 consumption and CO2 production in kinetic cells to delineate pyrite oxidation-carbonate buffering and microbial respiration in unsaturated media. J. Contam. Hydrol. 65 (3–4), 203–217. http://dx.doi.org/10.1016/S0169-7722(02)00248-6. September 2003.

Lottermoser, B.G., 2003. Mine Wastes: Characterization, Treatment and Environmental Impacts. Springer-Verlag, Berlin Heidelberg.

Maddocks, G., Lin, C., McConchie, D., 2004. Effects of Bauxsol and biosolids on soil conditions of acid-generating mine spoil for plant growth. Environ. Pollut. 127 (2), 157–167. http://dx.doi.org/10.1016/j.envpol.2003.08.001.

Mauric, A., Lottermoser, B.G., 2011. Phosphate amendment of metalliferous waste rocks, Century Pb-Zn mine, Australia. Appl. Geochem. 26 (1), 45–56. http://dx.doi.org/10.1016/j.apgeochem.2010.11.002.

McCarthy, T.S., 2011. The impact of acid mine drainage in South Africa. South Afr. J. Sci. 107 (5–6), 1–7. http://dx.doi.org/10.4102/sajs.v107i5/6.71.

McDonald, D.M., Webb, J.A., Taylor, J., 2006. Chemical stability of acid rock drainage treatment sludge and implications for sludge management. Environ. Sci. Technol. 40 (6), 1984–1990. http://dx.doi.org/10.1021/es0515194.

Mikhail, R.Sh, Abo-El-Enein, S.A., Hanafi, S., 1981. Ettringite formation in compressed expansive cement pastes. Cem. Concr. Res. 11 (5–6), 665–673. http://dx.doi.org/10.1016/0008-8846(81) 90025–9.

Miller, S., Smart, R., Andrina, J., Neale, A., Richards, D., 2003. Evaluation of limestone covers and blends for long-term acid rock drainage control at the Grasberg mine, Papua Province, Indonesia. In: Proceedings of the Sixth International Conference on Acid Rock Drainage, pp. 133–141. Cairns, Australia.

Miller, S., Schumann, R., Smart, R., Rusdinar, Y. (2009) ARD control by limestone induced armouring and passivation of pyrite mineral surfaces, Paper presented at Eighth International Conference on Acid Rock Drainage, June 23–26, Skellefta, Sweden.

Nieto, J.M., Sarmiento, A.M., Olias, M., Canovas, C.R., Riba, I., Kalman, J., Delvalls, T.A., 2007. Acid mine drainage pollution in the into and Odiel rivers (Iberian pyrite belt, SW Spain) and bioavailability of the transported metals to the Huelva Estuary. Environ. Int. 33 (4), 445–455. http://dx.doi.org/10.1016/j.envint.2006.11.010. May 2007.

Nordstrom, D.K., 2011. Mine waters: acidic to circumneutral. Elem. Dec. 2011 7 (6), 393–398. http://dx.doi.org/10.2113/gselements.7.6.393.

Nordstrom, D.K., Alpers, C.N., 1999. Negative pH, efflorescent mineralogy, and consequences for environmental restoration at the Iron Mountain Superfund site, California. Proc. Natl. Acad. Sci. U. S. A. 96 (7), 3455–3462 (Mar. 30, 1999).

Northwest Geochem, 1996. Evaluation of a Field Scale Application of a Shotcrete Cover on Acid Generating Rock. MEND project 2.34.1.

Parkhurst, D.L., Appelo, C.A.J., 2013. Description of input and examples for PHREEQC version 3—a computer program for speciation, batch-reaction, one-dimensional transport, and inverse geochemical calculations. U.S. Geol. Surv. Tech. Methods 6, A43.

Perez-Lopez, R., Nieto, J.M., de Almodovar, G.R., 2007. Utilization of fly ash to improve the quality of the acid mine drainage generation by oxidation of a sulphide-rich mining waste: column experiments. Chemosphere 67 (8), 1637–1646. http://dx.doi.org/10.1016/j.chemosphere.2006.10.009.

Ragnvaldsson, D., Bergknut, M., Lewis, J., Drotz, S., Lundkvist, A., Ambrahamsson, K., Fernerud, S., 2014. A novel method for reducing acid mine drainage using green liquor dregs. Environ. Chem. Lett. 12, 443–447. http://dx.doi.org/10.1007/s10311-014-0469-z.

Sahoo, P.K., Tripathy, S., Panigrahi, M.K., Equeenuddin, Sk.Md, 2013. Inhibition of acid mine drainage from a pyrite-rich mining waste using industrial by-products: role of neo-formed phases. Water, Air Soil Pollut. 224 (1757), 1–11. http://dx.doi.org/10.1007/s11270-013-1757-0.

Sariosseiri, F., Muhunthan, B., 2009. Effect of cement treatment on geotechnical properties of some Washington State soils. Eng. Geol. 104 (1–2), 119–125. http://dx.doi.org/10.1016/j.enggeo.2008.09.003.

Shabalala, A.N., Ekolu, S.O., Diop, S., Solomon, F., 2017. Pervious concrete reactive barrier for removal of heavy metals from acid mine drainage – column study. J. Hazard. Mater. 323 (Part B), 641–653. http://dx.doi.org/10.1016/j.jhazmat.2016.10.027.

Sheshpari, M., 2015. A review of underground mine backfilling methods with emphasis on cemented paste backfill. Electron. J. Geotechnical Eng. 20 (13), 5183–5208.

Skousen, J.G., Ziemkiewicz, P., Yang, J.E., 2012. Use of coal combustion by-products in mine reclamation: review of case studies in the USA. Geosystem Eng. 15 (1), 71–83. http://dx.doi.org/10.1080/12269328.2012.676258.

Song, Q., Yanful, E.K., 2010. Effect of water addition frequency on oxygen consumption in acid generating waste rock. J. Environ. Eng. 114 (1), 691–700. http://dx.doi.org/10.1061/(ASCE)EE.1943-7870.0000213.

Spence, R.D., 1987. Cost Estimate of Grouting the Proposed Test Pits at Idaho National Laboratory Using the ORNL-recommended Grouts. Oak Ridge National Laboratory. ORNL/TM-10025.

Stumm, W., Morgan, J.J., 1996. Aquatic Chemistry: Chemical Equilibria and Rates in Natural Waters, third ed. John Wiley & Sons, Inc.

Taylor, H.F.W., 1997. Cement Chemistry. Thomas Telford Publishing, London.

Taylor, G.F., Cox, R.C. (2003) The Brukunga pyrite mine- a field laboratory for acid rock drainage studies, Paper presented at Sixth International Conference on Acid Rock Drainage, Cairns, QLD, 12–18th July 2003.

Zumdahl, S.S., 1998. Chemical Principles- Third Edition. Houghton Mifflin Co., Boston, MA.